

Angular dependent light scattering from multicellular spheroids

J. R. Mourant

T. M. Johnson

V. Doddi

J. P. Freyer

Los Alamos National Laboratory

Bioscience Division

Los Alamos, New Mexico 87545

Abstract. We demonstrate that the effects of cell–cell contact and of changes in cell shape have only a minor effect on the angular distribution of light scattering from mammalian fibroblast cells. This result is important for the development of light scattering as a noninvasive tool for tissue diagnostics such as cancer detection. Changes in cell organization that are not accompanied by changes in internal cellular structure may not be measurable. On the other hand, changes in internal cellular structure should be measurable without interference from changes in overall cellular organization. The second major result of this work is that there are small but significant differences between light scattering of tumorigenic and nontumorigenic cells grown in a three-dimensional culture system. The cause of the differences in light scattering are likely due to the nontumorigenic cells arresting in the G1 phase of the cell cycle, while the tumorigenic cells continue to proliferate. © 2002 Society of Photo-Optical Instrumentation Engineers.

[DOI: 10.1117/1.1427053]

Paper 20057 received Nov. 30, 2000; revised manuscript received July 5, 2001; accepted for publication Sept. 6, 2001.

1 Introduction

Noninvasive light scattering methods have the potential to provide information on tissue and cell morphology for clinical diagnostic purposes. Pathologists have long used microscopic assessment of tissue morphology for diagnosis of cancer. Traditional methods, however, require that tissue be removed which puts significant limitations on tissue sampling. In addition, the taking of biopsy samples can be painful (sometimes requiring anesthesia), and can have side effects (including infection). Therefore, a noninvasive method that could provide *in vivo* information on cell morphology would have great utility. The scattering of light from tissue is expected to be sensitive to tissue and cellular structure. However, we do not yet know exactly what features of cells scatter light. There is growing evidence that most light scattering occurs from structures that are much smaller than the nucleus^{1–3} and that small changes in internal nuclear structures can cause significant changes in light scattering.⁴ Additionally, most of the light scattering properties of tissue can be reproduced with a broad distribution of spherical scatterers—the vast majority having a diameter less than 1 μm .⁵ The fact that most light scattering occurs from small intracellular structures raises the issue of whether measurements of light scattering are sensitive to cell shape and organization within multicellular structures. This paper address that issue.

Several clinical studies indicating that light scattering is sensitive to changes accompanying carcinogenesis have been published.^{6–11} Only a few of these papers attribute the changes in light scattering to a specific alteration in structure or biochemistry. It is very difficult to attribute a change in collected light intensity in tissue to a specific change, because epithelial tissue is structurally complicated and most light

scattering techniques probe beneath the cellular layer into the stroma. To simplify the problem, we examine light scattering from a well controlled carcinogenesis/tumorigenesis system. In previous work, we demonstrated that there are small light scattering differences between a pair of nontumorigenic and tumorigenic cell types grown under well controlled conditions.¹² In this work, we demonstrate differences in light scattering from two sets of tumorigenic and nontumorigenic cells grown in three-dimensional (3D) cell culture.

We use multicellular spheroids as an *in vitro* model of cellular tissue. Multicellular spheroids are spherical aggregates of tumor or normal cells and the extracellular matrix which they produce. They are a model system for the microenvironment of tumors and have been used to study the effects of microenvironmental stresses and cell–cell interactions on cellular proliferation, cellular viability, gene expression, metabolism, invasion, and response to numerous forms of cancer therapy.^{13–16} In this work we present results of angular dependent light scattering measurements of spheroids. These measurements are compared with angular dependent measurements of cells dissociated from the spheroids. By measuring the same cells in multicellular spheroids and after dissociation from multicellular spheroids we can determine the effects of cell–cell contact and intracellular matrix. Second, by examining spheroids of both tumorigenic and nontumorigenic cells, we can examine how the different microenvironment created by these cells in a three-dimensional environment affects light scattering properties.

2 Methods

2.1 Cell Culture

As an *in vitro* tumorigenesis model we have used two matched pairs of cells (M1/MR1 and Rat1/Rat1-T1) derived

Address all correspondence to Dr. Judith R. Mourant. Tel: 505-665-1190; Fax: 505-665-4637; E-mail: jmourant@lanl.gov

from a common rat embryo fibroblast (REF) cell line as described previously.¹⁷ M1 cells are an immortalized but nontumorigenic derivative of REF cells obtained through stable transfection with the c-myc oncogene. MR1 cells are a tumorigenic derivative of M1 cells obtained by stable transfection with a mutant h-ras oncogene: inoculation of nu/nu mice with MR1 cells results in rapid, invasive tumor growth with tumors reaching a volume $>10\text{ cm}^3$ in two weeks.¹⁷ Rat1 cells are a spontaneously immortalized version of REF cells which are also not tumorigenic. Tumorigenic Rat1-T1 cells are derived from Rat1 cells by stable transfection with the same mutant h-ras oncogene. All cells were maintained in monolayer culture using Dulbecco's modified minimal essential medium (Gibco) supplemented with 5% fetal bovine serum (Hyclone), α -D-glucose (16.5 mM), penicillin, and streptomycin, hereafter referred to as complete medium. Further details of monolayer cell cultures have been provided previously.^{12,18}

2.2 Spheroid Culture

Spheroids were initiated from exponentially growing monolayer cultures essentially as described previously.¹⁸ Briefly, a single-cell suspension was prepared from monolayer cultures by trypsinization and inoculated into complete medium in culture dishes with an underlayer of 0.5% agarose (Sigma Chemicals). Previous work has demonstrated that all four cell lines formed spheroids under these conditions, but the nontumorigenic cell lines (M1 and Rat1) arrested their proliferation while the tumorigenic cell lines (MR1 and Rat1-T1) continued to proliferate in aggregate culture.^{19,20} In order to obtain approximately equal numbers of cells per dish at the time of harvesting spheroids, 1×10^6 M1 or Rat1 cells were inoculated per 100 mm culture dish while only 2×10^5 MR1 or Rat1-T1 cells were inoculated per dish. The aggregates were cultured for four days then harvested by decanting the spheroid suspension from the dishes, gently pelleting the spheroids by centrifugation ($100 \times g$ for 3–4 min) and resuspending the spheroids in ice-cold calcium- and magnesium-free phosphate-buffered saline (PBS, Gibco).

2.3 Spheroid Size Analysis

An aliquot of the spheroid suspension was removed and the size distribution of the aggregates determined as described previously.⁶ Briefly, the major and minor orthogonal axes of 25 individual aggregates were measured using a calibrated reticule in an inverted microscope (Zeiss). The geometric mean diameter and total volume of each spheroid were determined from the axis measurements and population mean diameters and volumes were determined from the individual values.

2.4 Dissociation of Spheroids to Single Cells

After making angular-dependent light scattering measurements on intact spheroids, the aggregates were dissociated to a single-cell suspension, allowing for measurement of exactly the same cell culture under aggregated and single-cell conditions. Spheroids were dissociated as described previously.¹⁸ Briefly, the spheroid suspension was pelleted by centrifugation ($1000 \times g$ for 10 min), the PBS was decanted, 5 mL of a trypsinization solution [0.25% bovine trypsin (Gibco), 1 mM EDTA (Gibco), 25 mM HEPES (Sigma) in PBS at pH 7.4] was

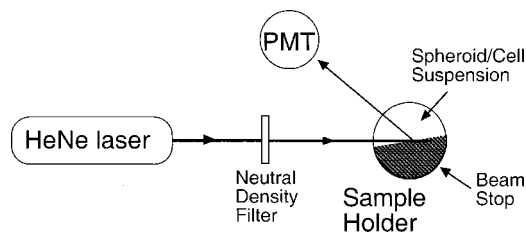


Fig. 1 Top view diagram of the instrumentation used to make angular dependent scattering measurements, where PMT indicates the photomultiplier tube.

added and the spheroids were incubated at 37°C for 10 min with occasional vortexing. After incubation, 10 mLs of ice-cold complete medium was added and the suspension was mixed by passing through a pipet ten times. The resulting single-cell suspension was then pelleted ($1000 \times g$ for 10 min), the medium/trypsin solution was decanted and the cells were resuspended in 50 mL of ice-cold PBS for light scatter analysis.

2.5 Cell Counting and Cell Volume Analysis

After dissociation from spheroids an aliquot of each cell suspension was counted using an electronic particle counter interfaced to a pulse-height analyzer (Coulter Electronics). Three counts were made of each suspension and averaged. During counting a cell volume distribution was accumulated using the pulse-height analyzer and the mean cell volume was computed.

2.6 Cell Cycle Analysis

Determination of the cell cycle distribution of the cells obtained from spheroids was performed using flow cytometric DNA content analysis as described in detail previously.¹⁸ Briefly, an aliquot of 10^6 cells from the single-cell suspension obtained from spheroids was fixed in 70% ethanol and stored in a refrigerator. Fixed samples were prepared for analysis by centrifuging the cells to a pellet ($1000 \times g$ for 10 min), decanting the ethanol and resuspending the cells in 1 mL of a DNA staining solution containing $50\ \mu\text{g/mL}$ propidium iodide (Sigma) and 100 units/mL RNase (Sigma) in PBS with calcium and magnesium (Gibco). Cells were incubated in the staining solution overnight at 4°C . DNA content analysis was performed on a FACS Calibur (Becton-Dickenson) flow cytometer using 488 nm excitation and fluorescence collection with the propidium iodide filter set. DNA content histograms containing 10^4 cells were collected which had coefficients of variation on the G1-phase peak of $<4\%$. Histograms were analyzed for cell cycle distribution with the MacCycle program (Phoenix Flow Systems) using the debris and aggregate elimination options.

2.7 Angular Dependent Scattering Measurements

For measurement of angular dependent light scattering, cells and spheroids were suspended in 50 mL of saline. The cell concentrations varied between 9×10^4 and 9×10^5 cells per mL. The experimental apparatus used for measuring angularly resolved light scattering is shown in Figure 1. Briefly, an unpolarized HeNe laser (Uniphase, Inc.) was incident on a sus-

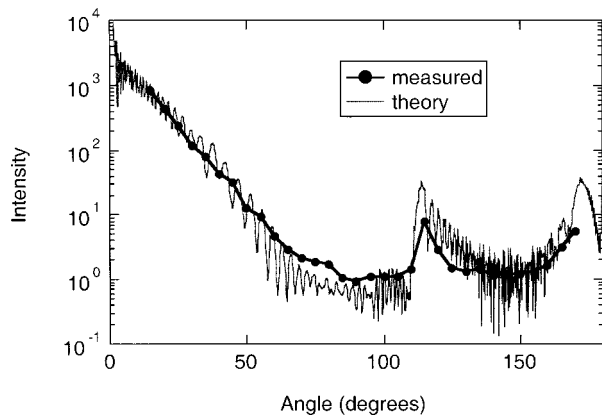


Fig. 2 Angular dependent light scattering of polystyrene spheres with a diameter of $98.5 \mu\text{m}$ compared to theoretical predictions computed using MIE theory.

pension of cells and the scattered light was measured with a photomultiplier tube (Hamamatsu, Inc.) which could be rotated around the sample cell. To obtain the dynamic range necessary for the experiment, neutral density filters were placed in front of the laser. Two different sample cells were used. The one depicted in Figure 1 contains a beam stop to reduce reflection from the glass container that can interfere with measurements of high angle scatter. The other sample cell consists of a simple glass cylinder on a base and was used for measuring scattering at angles of 45° and smaller. Data are usually obtained between $\sim 6^\circ$ and 170° . The most reliably high quality data are obtained between 15° and 160° . Systematic errors due to stray light scattering are very difficult to

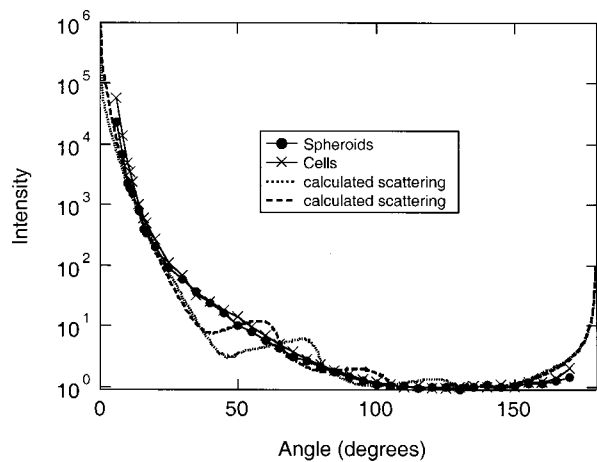
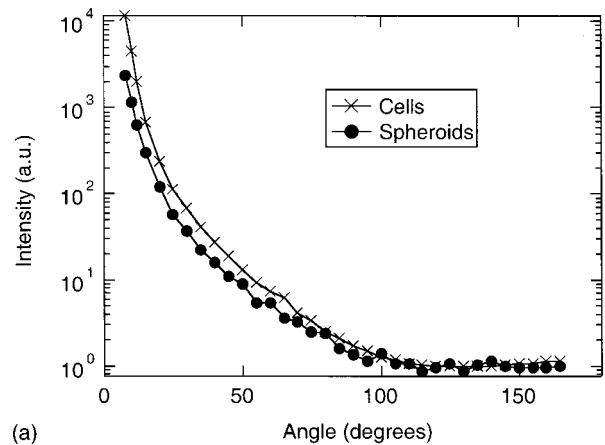
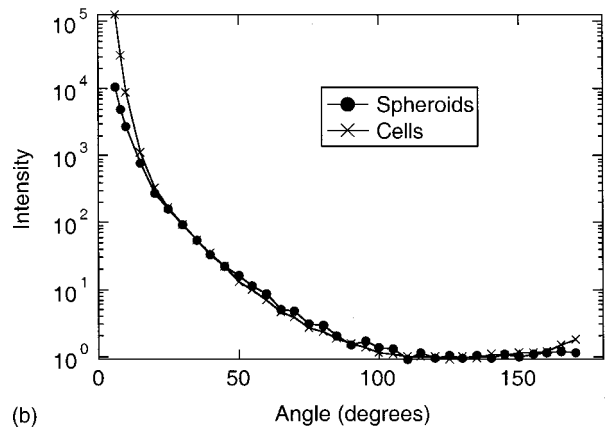


Fig. 3 Angular dependent light scattering from separate suspensions of MR1 cells and multicellular MR1 spheroids. The symbols (circles for spheroids, crosses for cells) are measurement results and the lines connect the measurement points. For the spheroids each symbol is the result of averaging three readings. For the cells only one reading was taken for each measurement point. The dashed and dotted lines are the results of MIE theory calculations for distributions of spheres. The sphere size distribution was assumed to be Gaussian with a mean of $76 \mu\text{m}$ and a standard deviation of $20 \mu\text{m}$. The dashed line is the result of averaging the results for sphere indices of 1.36, 1.37, 1.38 and 1.39 all in a medium of index of 1.33. The dotted line is the result of averaging results for sphere indices ranging from 1.37 to 1.43.



(a)



(b)

Fig. 4 (a) Angular dependent light scattering from suspensions of Rat1-T1 cells and multicellular Rat1-T1 spheroids. The data are presented as described in Figure 3. (a) Data set in which the difference between cells and spheroids was the greatest. (b) Data set in which this difference was the smallest.

avoid at angles greater than 160° . To assure that the system was giving accurate results, measurements of polystyrene spheres were compared to theory. Figure 2 demonstrates reasonable agreement between the theory and measurement for polystyrene spheres of $98.5 \mu\text{m}$ diameter.

Angular dependent light scattering intensities from M1 and MR1 cells and multicellular spheroids were determined on four separate days spaced weeks apart. On each day M1 cells and multicellular spheroids, and MR1 cells and multicellular spheroids were measured. Rat1 and Rat1-T1 cells and spheroids were measured in the same manner on five separate days.

3 Results

The results of angular dependent light scattering measurements of MR1 spheroids and of the cells subsequently dissociated from these spheroids are shown in Figure 3. The data have been normalized such that the integrated intensity from 120° to 150° is the same for the spheroids and the cells. This angle range was chosen because the errors in measurement are small over this angle range and the intensity does not vary greatly. Figure 3 indicates that the dependencies of light scattering on angle for the MR1 spheroids and the cells obtained

Table 1 Comparison of scattering properties for suspensions of cells and multicellular spheroids.

	M1	MR1	Rat1	Rat1T1
$I_{fs}(\text{cells})/ I_{fs}(\text{spheroids})$	1.41±0.78	1.07±0.36	1.2±0.3	1.9±0.8
$I_{bs}(\text{cells})/ I_{bs}(\text{spheroids})$	1.11±0.21	1.08±0.16	1.07±0.04	1.14±0.09

by dissociating the spheroids are very similar. This similarity in shapes of the angular dependent light scattering measurements also held for the M1 spheroids and M1 cells as well as the Rat1 spheroids and Rat1 cells. The measurements of the Rat1-T1 cells and multicellular spheroids, however, were more variable. In some cases the angular dependence of light scattering was the same for the cells and the spheroids, in other cases there were significant differences. In Figure 4 two sets of cell and spheroid data are plotted. The ones in Figure 4(a) show the largest difference observed for Rat1-T1 cells and spheroids while the measurements in Figure 4(b) are the most similar measurements of Rat1-T1 cells and spheroids.

To quantify some of the more subtle features of the angular dependent light scattering measurements, we integrated the scattered light intensity over the angle range 15°–35°. This integrated intensity, I_{fs} , will be greater when there is relatively more forward scattering (fs). We compared the amount of forward scattering from the cells and the spheroids by taking the ratio of I_{fs} for the paired cells and spheroids. The results are given in Table 1. The errors given are the standard deviation of the ratios. On average the cells have relatively more forward scattering than the spheroids. However, there are not sufficient data to show that the ratio of forward scattering is significantly different from one. We also noticed that there was a small upturn at high angles for the measurements of cells. To quantify this result, the intensities of the normalized angular dependent light scattering measurements were integrated for angles greater than 150° to indicate the intensity of backscatter, I_{bs} . The results given in Table 1 show a trend towards an increase in high angle scattering for the cells compared to the spheroids. However, with the present amount of data (four to five measurements of each cell type) the ratio is not statistically different from one.

A pairwise comparison was then performed of tumorigenic and nontumorigenic spheroids measured on the same day and of tumorigenic and nontumorigenic cells measured on the

Table 3 The averages and standard deviations for cell cycle analysis of the measurements of DNA content.

	M1	MR1	Rat1	Rat1-T1
% cells in G1	93.2 ± 2.3	63.9±8.2	84.1 ± 5.9	56.7±5.3
% cells in S	4.8 ± 1.9	24.8±1.7	6.4 ± 2.4	29.5±2.8
% cells in G2	1.9 ± 0.8	11.2±6.7	9.4 ± 6.5	13.7±4.8

same day. The relative intensity of forward scattering, I_{fs} , of the nontumorigenic suspensions divided by the intensity of forward scattering, I_{fs} , of the tumorigenic suspensions is given in Table 2. There is a trend for the nontumorigenic cells to have relatively more forward scattering than the tumorigenic cells. For the spheroids, the forward scattering is significantly greater from the nontumorigenic than from the tumorigenic spheroids.

Cell cycle analyses were performed for most of the measured cell suspensions. The percentages of cells in the S phase of the cell cycle were much greater for the tumorigenic than the nontumorigenic cells as can be seen from Table 3. Conversely, the percentage of cells in the G1 phase of the cell cycle was greater for the nontumorigenic than the tumorigenic cells. Cell counts taken at the time of preparing cell suspensions showed that the tumorigenic cells increased in number by 30-fold over the four day culture period, while the nontumorigenic cell cultures did not significantly increase in number. This is consistent with previous work,^{19,20} and, in conjunction with the cell cycle data, indicates that the tumorigenic cells were proliferating while the nontumorigenic cells were arrested in their cell cycle progression.

The sizes of the spheroids were determined by microscopic analysis as described in the methods section. The mean diameter and standard deviation of the mean diameter are given in Table 4. In each suspension of spheroids there was a large distribution of sizes, with coefficients of variation of the spheroid diameter distribution within one population of 15%–20%.

The probability of multiple scattering events within a spheroid can be estimated assuming a spheroid diameter of 76 μm and a scattering coefficient of 100 cm⁻¹, which is typical of tissue. The average number of scattering events is then 0.76. Employing the Poisson distribution, we find that for a photon traversing the center of the spheroid, the probability of not scattering is 0.467, the probability of exactly one scatter-

Table 2 The relative intensity of forward scattering from suspensions of nontumorigenic spheroids and cells divided by the relative intensity of forward scattering from suspensions of tumorigenic cells and multicellular spheroids. Ratio were calculated for each measurement pair. The average and standard deviation of these results is shown in the table. The two right hand columns are the average and standard deviation of all of the measurements regardless of whether they were of cells or multicellular spheroids.

	Spheroids		Cells		Cells and spheroids	
	Rat1/Rat1T1	M1/MR1	Rat1/Rat1T1	M1/MR1	Rat1/Rat1T1	M1/MR1
$I_{fs}(\text{nontumorigenic})/ I_{fs}(\text{tumorigenic})$	1.76±0.39	1.33±0.26	1.13±0.51	1.44±0.49	1.41±0.55	1.39±0.38

Table 4 The averages and standard deviations of the mean spheroid diameters determined by microscopic analysis.

	M1	MR1	Rat1	Rat1T1
Range of average spheroids diameters	$72 \pm 5 \mu\text{m}$	$89 \pm 5 \mu\text{m}$	$69 \pm 8 \mu\text{m}$	$92 \pm 16 \mu\text{m}$

ing events is 0.355, the probability of exactly two scattering events is 0.135, the probability of exactly three scattering events is 0.034, etc. In our analysis of the scattering data we have assumed that only single scattering events occur in the spheroids. This approximation is very reasonable because most scattering events cause only a very small deviation in the trajectory of the photon. On the rare occasions that there are multiple scattering events within a spheroid, it is very likely that one of them is a small angle scattering event causing a deviation of less than 20° . To determine how such multiple scattering events would degrade the resolution of our measurements, we smoothed the calculated angular light scattering intensities using a 40° -wide moving average. There was no effect at all for angles between 50° and 165° . The smoothing increased the intensity at angles below 50° . This increase was greatest at the smaller angles—at 10° there was a 35% increase in intensity.

To evaluate the possibility that for light scattering purposes the multicellular spheroids could be considered as homogeneous spheres, the scattering from a broad distribution of spheres was calculated. We used a Gaussian distribution with a mean of $76 \mu\text{m}$ and a standard deviation of $20 \mu\text{m}$ in agreement with our microscopic measurements. Calculations for this distribution were done assuming that the spheroids were homogeneous with refractive indices between 1.36 and 1.43 and were immersed in a medium of index 1.33. The thick dotted line in Figure 3 is the average of angular dependent scattering for indices of 1.36–1.39. The thick dashed line is the average for indices from 1.40 to 1.43. Both curves have been scaled to have the same integrated intensity from 120° to 160° as the experimental data. Several differences were found between the calculation results and the experimental measurements of spheroids. Despite using a broad distribution of scatterer sizes and refractive indices, ripples were seen in the calculations which were not present in the experimental result. Second, the relative amount of forward scattering was less at angles between 25° and 50° in the calculations, with the biggest differences in the 30° – 40° range. Finally, the calculations show a strong upturn at large angles. This increase in scattering at the highest angles was not observed in the experimental data.

A more sensitive test than unpolarized angular dependent light scattering for determining whether the multicellular spheroids scatter light like homogeneous spheroids is polarized light scattering. A dip in the scattered light intensity will appear near 90° if the scatterers are small (diameter of a few microns or less) but not if the primary scattering center is the size of the spheroids (i.e., $10 \mu\text{m}$ or larger). The results of polarized angular dependent light scattering measurements of multicellular spheroids and of cells dissociated from the multicellular spheroids are shown in Figure 5. The results of in-

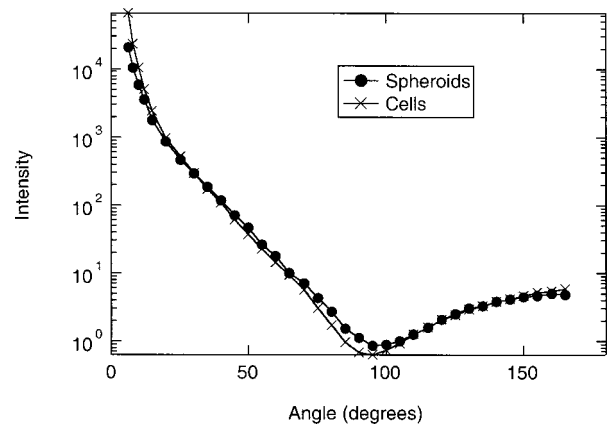


Fig. 5 Angular dependent polarized light scattering from separate suspensions of MR1 cells and multicellular MR1 spheroids. The light was polarized parallel to the scattering plane. The symbols (circles for spheroids, crosses for cells) are measurement results and the lines connect the measurement points. For the spheroids each symbol is the result of averaging three readings. For the cells only one reading was taken for each measurement point. The error in each measurement is about $1/3$ of the size of the symbol.

cident and detected light polarized parallel to the scattering plane are very similar for the cells and multicellular spheroids: in both cases there is a dip near 90° .

4 Discussion

In order for light scattering to be developed into a noninvasive tool for assessment of tissue morphology, it is important to have an understanding of what features of tissue scatter light. Previous work has provided evidence that light scattering occurs from small internal structures inside of cells.^{1,2,4,21} If internal structures are the primary cause of light scattering from cells in suspension, then altering cell shape or cell–cell contact per se should not change the light scattering properties unless such changes involve a concomitant change in internal cellular morphology.

In this work we have compared light scattering from suspensions of cells and suspensions of multicellular spheroids. In suspension the cells are spherical in shape. When grown in a multicellular spheroid, the cells take on a shape typical of that found in tissue and are no longer spherical. Therefore, if light scattering measurements were acutely sensitive to cell shape a large change in the scattering signal would be expected. For M1, MR1, and Rat1 cells we found no difference in the angular dependence of light scattering from the multicellular spheroids or the cells dissociated from the multicellular spheroids. For the Rat1-T1 cells, there was variation in our results; some measurements showed a significant difference between the scattering from cells and multicellular spheroids. The reason for this difference is not understood. The size of the spheroids, the size of the cells, and the cell cycle data were not significantly different in experiments where the Rat1-T1 cells and spheroids scattered differently than when the scattering was the same.

Although the angular dependence of light scattering from cells and multicellular spheroids was found to be very similar in most cases, there were some discernable differences. There was slightly more forward scattering from the cells than from

the multicellular spheroids. Earlier measurements of g for cells gave a value of 0.98.¹ A decrease in forward scattering will decrease the value of g bringing it closer to values which have been measured for tissue; ~ 0.94 for porcine liver,²² 0.96 for bovine muscle,²³ 0.94–0.965 for bovine muscle, pig brain, and white chicken muscle.²⁴ A small increase in scattering at the very highest angles was also observed for the cells as compared to the spheroids.

For the polarized measurements of spheroids there was a small difference between the position of the dip in scattered intensity of light polarized parallel to the scattering plane for the cells and for the multicellular spheroids. The dip shifts slightly to the higher angles indicating that the average effective scatterer size is slightly larger for the suspension of multicellular spheroids than for the suspension of cells. Comparison with MIE theory calculations provides an estimate of about 0.1 μm for the change in the average effective scatterer radius. Although these results are only for one set of MRI cells and spheroids, it demonstrates that the difference between the average effective scatterer sizes in the cells and spheroids must be small—on the order of 10^{th} s of microns or less. Also, consistent with the unpolarized measurements, the polarized measurements show a greater upturn at small angles for the cells than the multicellular spheroids.

In addition to the small differences noted between spheroids and cells, small differences were noted between scattering from multicellular spheroids of tumorigenic and nontumorigenic cells. For both the M1/MR1 cell pair and the Rat1/Rat1-T1 cell pair, there was relatively more forward scattering from multicellular spheroids composed of the nontumorigenic cells than from spheroids composed of tumorigenic cells. Because only relative measurements of light scattering were made and the data were normalized from 120° to 150° , the increase in relative forward scatter of the nontumorigenic cells could be stated as an increase in the relative backscatter of the tumorigenic cells. In multicellular spheroid culture, the tumorigenic cells replicate rapidly while the nontumorigenic cells are not replicating.²⁵ Our cell cycle analysis combined with knowledge of cell number at the start and end of spheroid culture showed clearly that the tumorigenic cells were replicating more rapidly than the nontumorigenic cells. The results that the rapidly replicating tumorigenic cells have relatively more backscattering than the non- or slowly replicating nontumorigenic cells is consistent with previous work reporting that rapidly growing cells have more backscattering than cells which are not rapidly replicating.²

5 Conclusions

The general similarity between scattering from cells in suspension and scattering from cells in multicellular spheroids indicates that cell shape and intercellular matrix are not controlling factors for light scattering from cells. The fact that cell shape has very little effect on light scattering does not mean that the microenvironment of the tissue is unimportant to determining scattering properties. MRI and Rat1-T1 cells, by nature of being tumorigenic, proliferate rapidly in 3D cell culture while their nontumorigenic counterparts M1 and Rat1 cells do not, consequently, the tumorigenic cells and spheroids have relatively more backscattering.

Acknowledgment

This work was supported by NIH NCI Grant No. CA71898.

References

1. J. R. Mourant, J. P. Freyer, A. H. Hielscher, A. A. Eick, D. Shen, and T. M. Johnson, "Mechanisms of light scattering from biological cells relevant to noninvasive optical tissue diagnostics," *Appl. Opt.* **37**, 3586–3593 (1998).
2. J. R. Mourant, M. Canpolat, C. Brocker, O. Esponda-Ramos, T. Johnson, A. Matanock, K. Stetter, and J. P. Freyer, "Light scattering from cells: The contribution of the nucleus and the effects of proliferative status," *J. Biomed. Opt.* **5**, 131–137 (2000).
3. J. R. Mourant, T. M. Johnson, and J. P. Freyer, "Characterizing mammalian cell and cell phantoms by polarized back-scattering fiber-optic measurements," *Appl. Opt.* (submitted).
4. R. Drezek, A. Dunn, and R. Richards-Kortum, "A pulsed finite-difference time-domain (FDTD) method for calculating light scattering from biological cells over broad wavelength ranges," *Opt. Express* **6**, 147–157 (2000).
5. J. M. Schmitt and G. Kumar, "Optical scattering properties of soft tissue: A discrete particle model," *Appl. Opt.* **37**, 2788–2797 (1998).
6. I. J. Bigio, S. G. Bown, G. Briggs, C. Kelley, S. Lakhani, D. Pickard, P. M. Ripley, I. G. Rose, and C. Saunders, "Diagnosis of breast cancer using elastic-scattering spectroscopy: Preliminary clinical results," *J. Biomed. Opt.* **5**, 221–228 (2000).
7. M. B. Wallace, L. T. Perelman, V. Backman, J. M. Crawford, M. Fitzmaurice, M. Seiler, K. Badizadegan, S. J. Shields, I. Itzkan, R. R. Dasari, J. van Dam, and M. S. Feld, "Endoscopic detection of dysplasia in patients with Barrett's esophagus using light-scattering spectroscopy," *Gastroenterology* **119**, 677–682 (2000).
8. J. R. Mourant, I. J. Bigio, J. Boyer, R. Conn, T. Johnson, and T. Shimada, "Spectroscopic diagnosis of bladder cancer with elastic light scattering," *Lasers Surg. Med.* **17**, 350–357 (1995).
9. J. R. Mourant, I. J. Bigio, J. Boyer, T. Johnson, and J. Lacey, "Detection of gastrointestinal cancer by elastic-scattering spectroscopy," *J. Biomed. Opt.* **1**, 192–199 (1996).
10. G. Zonios, L. T. Perelman, V. Backman, R. Manoharan, M. Fitzmaurice, J. Van Dam, and M. S. Feld, "Diffuse reflectance spectroscopy of human adenomatous colon polyps in vivo," *Appl. Opt.* **38**, 6628–6637 (1999).
11. V. P. Wallace, D. Crawford, P. S. Mortimer, R. J. Ott, and J. C. Bamber, "Spectrophotometric assessment of pigmented skin lesions: Methods for feature selection for evaluation of diagnostic performance," *Phys. Med. Biol.* **45**, 735–751 (2000).
12. J. R. Mourant, A. H. Hielscher, A. A. Eick, T. M. Johnson, and J. P. Freyer, "Evidence for intrinsic differences in light-scattering properties of tumorigenic and nontumorigenic cells," *Cancer Cytopathology* **84**, 366–374 (1998).
13. R. M. Sutherland, "Cell and environment interactions in tumor microregions: The multicell spheroid model," *Science* **240**, 177–184 (1988).
14. J. P. Freyer, "Spheroids in radiobiology research," in *Spheroid Culture in Cancer Research*, R. Bjerkvig, Ed., pp. 217–275, CRC, Boca Raton, FL (1992).
15. W. Mueller-Klieser, "3-dimensional cell cultures: From molecular mechanisms to clinical applications," *Am. J. Physiol. Cell Physiol.* **42**, C1109–C1123 (1997).
16. L. A. Kunz-Schughart, M. Kreutz, and R. Knuechel, "Multicellular spheroids: A 3-dimensional in vitro culture system to study tumor biology," *Int. J. Exp. Pathol.* **79**, 1–23 (1998).
17. L. A. Kunz-Schughart, A. Simm, and W. Mueller-Klieser, "Oncogene-associated transformation of rodent fibroblasts is accompanied by large morphologic and metabolic alterations," *Oncol. Rep.* **2**, 651–661 (1995).
18. J. P. Freyer, "Mitochondrial function of proliferating and quiescent cells isolated from multicellular tumor spheroids," *J. Cell Physiol.* **176**, 138–149 (1998).
19. L. A. Kunz-Schughart, K. Groebe, and W. Mueller-Klieser, "Three-dimensional cell culture induces novel proliferative and metabolic alterations associated with oncogenic transformation," *Int. J. Cancer* **66**, 578–586 (1996).
20. K. E. LaRue, M. E. Bradbury, and J. P. Freyer, "Regulation of G1 transit by cyclin kinase inhibitors in multicellular spheroid cultures of

- rat embryo fibroblast cells transformed to different extent," *Cancer Res.* **58**, 1305–1314 (1998).
21. R. Drezek, A. Dunn, and R. Richards-Kortum, "Light scattering from cells: Finite-difference time-domain simulations and goniometric measurements," *Appl. Opt.* **38**, 3651–3661 (1999).
 22. A. Roggan, D. Schadel, U. Netz, J.-P. Ritz, C.-T. Germer, and G. Muller, "The effect of preparation technique on the optical parameters of biological tissue," *Appl. Phys. B: Lasers Opt.* **69**, 445–453 (1999).
 23. J. R. Zijp and J. J. tenBosch, "Optical properties of bovine muscle tissue in vitro; a comparison of methods," *Phys. Med. Biol.* **43**, 3065–3081 (1998).
 24. S. T. Flock, B. C. Wilson, and M. S. Patterson, "Angular dependence of HeNe laser light scattering by dermis," *Lasers Life Sci.* **1**, 309–333 (1987).
 25. S. Walenta, J. Doetsch, W. Mueller-Klieser, and L. Kunz-Schughart, "Metabolic imaging in multicellular spheroids of oncogene-transfected fibroblasts," *J. Histochem. Cytochem.* **48**, 509–522 (2000).